Sequestration of CO_2 in geological media in response to climate change: capacity of deep saline aquifers to sequester CO_2 in solution

S. Bachu [*], J.J. Adams

Alberta Geological Survey, Alberta Energy and Utilities Board, 4999-98 Avenue 4th Floor, Twin Atria, Edmonton, AB, T6B 2X3, Canada

Abstract

Geological sequestration is a means of reducing anthropogenic atmospheric emissions of CO_2 that is immediately available and technologically feasible. Among various options, CO_2 can be sequestered in deep aquifers by dissolution in the formation water. The ultimate CO_2 sequestration capacity in solution (UCSCS) of an aquifer is the difference between the total capacity for CO_2 at saturation and the total inorganic carbon currently in solution in that aquifer, and depends on the pressure, temperature and salinity of the formation water. Assuming non-reactive aquifer conditions, the current carbon content is calculated using standard chemical analyses of the formation waters collected by the energy industry on the basis of the concentration of carbonate and bicarbonate ions. Formation water analyses performed at laboratory conditions are brought to in situ conditions using a geochemical speciation model to account for dissolved gasses that are lost from the water sample. To account for the decrease in CO_2 solubility with increasing water salinity, the maximum CO_2 content in formation water is calculated by applying an empirical correction to the CO_2 content at saturation in pure water. The UCSCS in an aquifer is calculated by considering the effect of dissolved CO_2 on the formation water density, the aquifer thickness and porosity to account for the volume of water in the aquifer pore space and for the mass of CO_2 dissolved in the water currently and at saturation. The methodology developed for estimating the ultimate CO_2 sequestration capacity in solution in aquifers has been applied to the Viking aquifer in the Alberta basin in western Canada. Considering only the region where the injected CO_2 would be a dense fluid, the capacity of the Viking aquifer to sequester CO_2 in solution in the formation water is calculated to be 100 Gt. Simple estimates then indicate that the capacity of the Alberta basin to sequester CO_2 dissolved in the formation waters at depths greater than 1000 m is on the order of 4000 Gt CO_2. The results also show that using geochemical models to bring the analyses of the formation waters to in situ conditions is not warranted

[*] Corresponding author. Tel.: +1-780-422-1927; fax: +1-780-422-1459/427-1517.
E-mail address: stefan.bachu@gov.ab.ca (S. Bachu).

when the current total inorganic carbon (TIC) in the aquifer water is very small by comparison with the CO_2 solubility at saturation. Furthermore, in such cases, the current TIC may even be neglected.

1. Introduction

Atmospheric concentrations of greenhouse gases, such as carbon dioxide (CO_2) and methane (CH_4), have increased since the industrial revolution to the point that significant climate warming and weather changes have been attributed to anthropogenic activity [1,2]. Of all the other greenhouse gases, CO_2 is responsible for about 64% of the enhanced 'greenhouse effect', making it the target for mitigation of greenhouse gases [1]. Atmospheric concentrations of CO_2 have risen from pre-industrial levels of 280–360 ppm [1], primarily as a consequence of fossil fuel combustion for energy production. Fossil fuels, which today provide about 75% of the world's energy, are likely to remain a major component of the world's energy supply for at least the next century because of their inherent advantages, such as availability, competitive cost, ease of transport and storage and large resources [2,3]. Thus, a major challenge in mitigating the anthropogenic effects on climate change is the reduction of CO_2 emissions within or outside the framework of the Kyoto Protocol.

Reducing anthropogenic CO_2 emissions into the atmosphere basically involves three approaches, which are best expressed by the following relationship between carbon emissions (C), energy (E) and economic growth as measured by the gross domestic product (GDP):

$$\text{Net } C = \text{GDP} \times (E/\text{GDP}) \times (C/E) - S \tag{1}$$

where E/GDP is the 'energy intensity' of the economy, C/E is the 'carbon intensity' of the energy system and S represents the carbon removed from the atmosphere (carbon 'sinks'). The product of the energy intensity of the economy and the carbon intensity of energy production is the carbon, or emission, intensity of the economy (C/GDP).

Historical evidence shows that the emission intensity has decreased continuously since the beginning of the industrial revolution, the carbon removed from the atmosphere (S) has decreased slightly as a result of deforestation and agricultural practices and the net carbon emissions (C) have increased, mainly as a result of increasing economic growth (GDP), which has surpassed the decrease in emission intensity. Thus, a reduction in net CO_2 emissions into the atmosphere can be achieved by: (1) lowering the energy intensity (E/GDP) of the economy by increasing the efficiency of primary energy conversion and end use, (2) lowering the carbon intensity (C/E) of the energy system by substituting lower carbon or carbon free energy sources for the current sources and (3) artificially increasing the capacity and capture rate of the carbon sinks.

It is recognized that no single category of mitigation measures is sufficient [4]. However, increasing the amount of carbon removed from the atmosphere is the most viable at this time. The energy intensity of the economy will continue to decrease at a lower rate than that of the increase in GDP, and technology based mitigation strategies will have a limited impact on reducing CO_2 emissions into the atmosphere unless revolutionary, large scale technological advances and major

expenditures occur in the near future. Similarly, the carbon intensity of the energy system is not likely to decrease in any significant way in the medium term because of the continuing use of fossil fuels as the primary energy source [3]. This leaves the increase in the number of carbon sinks (S) and of their capture rate as the only significant means of reducing net carbon emissions into the atmosphere in the short term [4].

A reduction of CO_2 emissions into the atmosphere can be achieved by enhancing natural, diffusive sinks, such as terrestrial ecosystems (soils and vegetation) and oceans, and creating artificial sinks at the bottom of the ocean and in geological media. The natural CO_2 sinks have CO_2 retention times of approximately tens to hundreds of years [5,6]. Although the capacity, but not the capture rate, of terrestrial ecosystems can be increased by changing forestry and agricultural practices, the net gain in stored carbon is uncertain and most likely less than initially thought [7]. In addition, competition from other land uses due to continuing population growth may severely limit the enhancement of terrestrial CO_2 sinks. The natural, diffuse and slow exchange of CO_2 between the atmosphere and the oceans can be artificially enhanced at discrete locations by injecting CO_2 to great depths, where it will form either hydrates or heavier than water plumes that sink to the ocean floor [8]. Ocean CO_2 storage, however, is hampered by high cost, technology development, potentially high environmental impact and a poor understanding of the associated physical and chemical processes. In addition, significant legal, political and international barriers may preclude large scale ocean disposal of CO_2. In contrast, geological storage and/or sequestration of CO_2 currently is likely to provide the first large scale opportunity for concentrated sequestration of CO_2 because the technology already exists, has been already implemented, albeit for different reasons, and the sequestration will be within national boundaries. From a technological point of view, all forms of CO_2 sequestration and storage can be immediately implemented because the technology for deep injection of CO_2, acid gases (CO_2 and H_2S) and industrial liquid waste is well established and currently in use, mainly by the energy and petrochemical industries [9–12]. Therefore, geological storage and/or sequestration of CO_2 represents the best short to medium term option for significantly enhancing CO_2 sinks, thus reducing net carbon emissions into the atmosphere. In this context, *geological sequestration and storage are defined as the removal of CO_2 directly from anthropogenic sources (capture) and its disposal in geological media, either permanently (sequestration) or for significant time periods (storage)*.

Carbon dioxide can be geologically sequestered in sedimentary basins, which are serendipituously associated with fossil fuels [13], by the following mechanisms: (1) stratigraphic and structural trapping in depleted oil and gas reservoirs, (2) solubility trapping in reservoir oil and formation water, (3) adsorption trapping in uneconomic coal beds, (4) cavern trapping in salt structures and (5) mineral immobilization [14–18]. All these trapping mechanisms, achievable through CO_2 injection, lead to carbon sequestration because the CO_2 is not returned to the atmosphere unless it is produced. The following actually represent forms of both geological sequestration and storage because a significant proportion of the injected CO_2 is produced at the pump and has to be captured, separated and re-circulated into the system: enhanced oil and gas recovery (EOR and EGR) [19,20] and enhanced coalbed methane recovery (ECBMR) [21,22]. Hydrodynamic trapping in deep aquifers [23] is also a form of both sequestration and storage because ultimately the carbon is released into the atmosphere at aquifer discharge, unless it had dissolved in the formation water. The retention time of these forms of CO_2 sequestration and storage varies between a few months to potentially millions of years, depending on flow paths and processes.

Of the many forms of CO_2 storage and sequestration in geological media, the economic benefits of producing additional oil or gas makes CO_2 sequestration and storage in EOR, EGR and ECBMR operations most likely to be implemented first. However, the total amount that can ultimately be sequestered in EOR operations is only a fraction of CO_2 emissions [24], whereas sequestration of CO_2 in depleted oil and gas reservoirs provides more capacity [25]. Because many oil and gas reservoirs are still producing and are not immediately available, this option will likely extend over a long period of time but will not provide sufficient capacity in the short to medium term. Sequestration in salt caverns is not likely to be implemented, except maybe for some very specific cases, because of its high cost. Compared with the previous options, sequestration of CO_2 in deep saline aquifers is considered as having, by far, the largest potential capacity, of the order of 1000 Gt [6], because of the extremely large volume of pore space in sedimentary basins. Although it does not bring an economic benefit, it is also likely to be implemented early on because it provides the necessary capacity and, in some instances, because of its availability and accessibility, as is the case of the Utsira Formation in the North Sea basin [26].

To date, capacity estimates for CO_2 sequestration in deep saline aquifers have been either very qualitative, being based on very simple assumptions and "back of the envelope" or "global" methods, or very local in scale, being based on reservoir scale numerical simulations. In this paper, we present the approach and methodology for quantitative assessment of the capacity of an aquifer to sequester CO_2 dissolved in the formation water, with an example of application to the Viking aquifer in the Alberta basin, Canada.

2. Ultimate CO_2 sequestration capacity in solution

Deep saline aquifers, which represent a significant portion by volume of sedimentary basins, can sequester or store carbon dioxide by three main mechanisms: (a) solubility trapping through dissolution in the formation water; (b) mineral trapping through geochemical reactions with the aquifer fluids and rocks and (c) hydrodynamic trapping of a CO_2 plume. In addition, a CO_2 plume may be trapped in structural and/or stratigraphic traps along the flow pathway, other than and including associated oil and gas reservoirs. Thus, the capacity of a deep saline aquifer can be considered for free-phase CO_2 in the pore space, dissolved phase CO_2 in formation water and CO_2 converted to rock matrix.

These three mechanisms for storage/sequestration of CO_2 operate on different time scales and have different degrees of permanency. Mineral trapping permanently removes CO_2 from the atmosphere as a result of mineral precipitation, assuming that no significant mineral changes occur afterwards in the system, but research so far has indicated that this is an extremely slow process [16]. A plume of free phase CO_2, even if it is flowing and dispersing in an aquifer driven by its own buoyancy and aquifer hydrodynamics, has an extremely long residence time, and it is effectively trapped within the flow system (hydrodynamic trapping) if the flow of formation water and of CO_2 is very slow, of the order of 10^{-3} to 10^{-2} m/yr [23], as is the case in most sedimentary basins. Because the flow is a dynamic process, the concept of hydrodynamic trapping is based on the time scale of the process, rather than on sequestration permanency. Thus, mineral and hydrodynamic trapping are, respectively, forms of CO_2 sequestration and storage. Solubility trapping has an intermediate character between mineral and hydrodynamic trapping in that, once CO_2 is dissolved

in the formation waters, it will travel, driven only by aquifer hydrodynamics without the possibly significant enhancement of its own buoyancy. If CO_2 saturated formation waters reach shallower depths, CO_2 may exsolve as a result of the associated decrease in pressure, although the concurrent decrease in temperature may counteract or reduce this effect. For deep saline aquifers in sedimentary basins, where flow velocities are of the order of 10^{-2} m/yr, the time scale of solubility trapping is at least of the same order of magnitude as the time scale of the basin scale flow processes.

Basically two approaches, leading to different results, have been used previously to estimate the CO_2 sequestration capacity of an aquifer other than through mineral immobilization. The "reservoir engineering" approach assumes that the injected CO_2, in separate phase, simply displaces the formation water in the pore space, similar to the oil displacement in a CO_2 flood enhanced oil recovery operation. The displaced water flows into a surrounding infinite aquifer, which theoretically, should "overflow" at aquifer discharge. Capacity estimates are based on local, reservoir scale numerical simulations of CO_2 injection that indicate an occupancy of the pore space by CO_2 on the order of a few percent as a result of gravity segregation and viscous fingering [27–32]. However, even in some of these simulations, it is assumed that CO_2 is soluble in water, with solubility varying between 3% and 10% depending on pressure. The simulations show that depending on simulation time scale and flow distance, a significant amount of the injected CO_2 will dissolve in the formation water at the edge of the CO_2 plume, an amount that can vary between 30% for flow at the reservoir scale [31] and 100% for flow at the basin scale [33]. Earlier on, Holt et al. [34] used an oil reservoir model and arrived at the conclusion that the amount of CO_2 stored in solution (~2% pore volume equivalent) is negligible by comparison with the amount of CO_2 stored as a separate phase (~30% pore volume). These seemingly contradictory results are the product of simulations performed at different spatial and temporal scales.

The other approach considers that dissolution is the primary method of CO_2 sequestration, and the capacity estimates are based on simple volumetric assumptions. Koide et al. [35] used the areal method of projecting natural resources reserves and assumed that 1% of the total area of the world sedimentary basins could be used for CO_2 sequestration. Other studies considered that 2–6% of the aquifer area can be used for CO_2 sequestration [36,37]. Capacity calculations then consider a CO_2 density of 40–60 kg CO_2/m^3 solution [34,38]. To date, both the displacement and dissolution approaches have considered only non-reactive conditions (i.e. no geochemical reactions take place concurrent with CO_2 injection, flow and dissolution).

A more realistic and rigorous approach is to consider that the injected CO_2 will dissolve in the formation waters up to saturation, and that mineral precipitation will take place concurrently or after saturation, depending on local conditions and the kinetics of the processes involved. The injected CO_2 in excess of saturation and/or precipitation will continue to flow as a separate phase in a plume, driven by buoyancy and aquifer hydrodynamics until it eventually either exhausts itself or leaks back into the atmosphere, even if after thousands to millions of years. Accordingly, the *maximum, or ultimate, potential* capacity of aquifers for CO_2 sequestration is the sum of their capacities for solubility trapping and for mineral precipitation.

Assuming that CO_2 dissolution is relatively much faster than carbonate precipitation [16], it is possible to decouple the two processes and consider only solubility trapping as the main mechanism for CO_2 sequestration in aquifers in the short to medium term (i.e. non-reactive physical processes control the CO_2 sequestration capacity). Thus, the Ultimate CO_2 Sequestration

Capacity in Solution (UCSCS) of an aquifer is the difference between the ultimate capacity and the current carbon content in solution in that aquifer. The ultimate capacity for CO_2 in solution in an aquifer is defined as the total amount of CO_2 that can theoretically dissolve to saturation in the formation water of that aquifer and be permanently trapped in a state of equilibrium, and it will not be released back into the atmosphere unless the aquifer water is produced or discharges naturally at the surface where the CO_2 will exsolve. The *current carbon content* represents the amount of inorganic carbon currently in solution in the formation waters as a result of natural geological processes.

Mathematically, the UCSCS is expressed by:

$$\text{UCSCS} = \iiint \varphi(\rho_S X_S^{CO_2} - \rho_0 X_0^{CO_2}) \, dx \, dy \, dz \qquad (2)$$
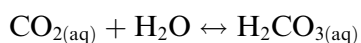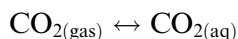
where φ is porosity, ρ is the density of the formation water, X^{CO_2} is the carbon content (mass fraction), and the subscripts 0 and S stand for current carbon content and at saturation, respectively. The mass fraction of CO_2 at saturation, $X_S^{CO_2}$, is a function of the formation water salinity, temperature and pressure. In this formulation, it is assumed that the pore space is water saturated ($S_w = 1$).
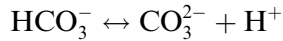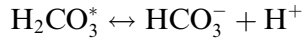
To calculate UCSCS, there is need to know the aquifer geometry (depth and thickness as functions of location) and porosity φ, pressure P, temperature T, water density and current CO_2 saturation at every point in the aquifer (functions of x, y and, sometimes, z if the aquifer is thick). For sedimentary basins, the aquifer geometry and water properties are not known in detail. However, based on data usually collected by the energy industry in the process of hydrocarbon exploration and production (i.e. stratigraphic picks, core analyses, bottom hole temperatures, formation water analyses and drill stem tests), it is possible to determine the aquifer geometry, porosity, temperature, salinity (total dissolved solids, or TDS) and pressure [39]. Determination of the carbon content, current and at saturation, and of the formation water density for the same situations requires significant additional processing.

3. Current carbon content

Ideally, the total inorganic carbon content of formation water should be measured for in situ conditions. In a basin setting, the in situ measurement of water properties or composition is very difficult and rarely done. Formation water samples routinely taken by the petroleum industry are analyzed for major ions at laboratory conditions but can be used to estimate the total inorganic carbon content in an aquifer. In a deep saline aquifer, an aqueous inorganic carbon system is primarily controlled by the dissolved CO_2 in the water and interaction with carbonate and siliciclastic minerals.

In general, atmospheric or subsurface CO_2 dissolves in water and generates a weak carbonic acid, which subsequently dissociates into HCO_3^- and CO_3^{2-} according to the following reactions:

$$CO_{2(gas)} \leftrightarrow CO_{2(aq)}$$

$$CO_{2(aq)} + H_2O \leftrightarrow H_2CO_{3(aq)}$$

$$H_2CO_3^* \leftrightarrow HCO_3^- + H^+$$

$$HCO_3^- \leftrightarrow CO_3^{2-} + H^+$$

where, by convention, the dissolved CO_2 and the carbonic acid are lumped together and denoted by $H_2CO_3^*$.

At the elevated temperatures and pressures found in a deep aquifer, the many dissolved solids in the water and a variety of mineral species result in complex chemical systems. To quantify this type of system, measurements of the total inorganic carbon (TIC), pH, temperature and pressure in the aquifer, along with a complete chemical water analysis and mineralogical characterization of the aquifer, are required to establish the existing species and buffering capacity of the water. Characterization of the system would facilitate prediction of the impact of any perturbation applied to the system, such as the introduction of CO_2 into a naturally reactive aquifer, which could cause dissolution–precipitation reactions, pH changes and speciation shifts.

No direct in situ measurements of total inorganic carbon or pH have been documented, and complete water and mineralogical analyses are usually done only for small study areas within a sedimentary basin. The limited amount of data hinders a detailed, basin wide study of CO_2 capacity. The lack of complete chemical analyses that quantify the minor species, which act as buffers, in the water requires that two assumptions be made to calculate TIC practically: *no non-carbonate buffers exist in the system* and *the disposal reservoir is non-reactive*. These two assumptions mean that the alkalinity or acid buffering capacity is controlled only by carbonate species and that addition of CO_2 to a system will cause the amount of carbon to increase, but no dissolution or precipitation of carbonate minerals will occur. These assumptions will generate a conservative estimate of capacity if non-carbonate buffers truly exist in the water. However, if only carbonate species control the pH, then the opposite is true. The capacity will be overestimated because the addition of CO_2 to an aquifer will result in dissolution of carbonate minerals, thereby reducing the available capacity for further dissolved CO_2 in the water. The benefit of these assumptions is that the capacity calculation is simplified to the difference between the maximum solubility of CO_2 and the existing total inorganic carbon in the formation water.

Thus, for non-reactive conditions, the total carbon content, C_T, which is the sum of these species, can be calculated according to:

$$C_T = (H_2CO_3^*) + (HCO_3^-) + (CO_3^{2-}) \tag{3}$$

where ( ) denotes concentration.

The concentration of bicarbonate and carbonate ions (HCO_3^- and CO_3^{2-}) in the formation water is measured, but the concentrations of the dissolved CO_2 and carbonic acid are not. However, the concentration of $H_2CO_3^*$ can be estimated on the basis of the relations between the activity, denoted by [ ], of these species at equilibrium:

$$K_1 = [HCO_3^-] \cdot [H^+]/[H_2CO_3^*]$$

$$K_2 = [CO_3^{2-}] \cdot [H^+]/[HCO_3^-]$$

and the relations between concentration and activity for each species. The latter is of the form:

$$[X] = \gamma_X \cdot (X)$$

where X is any chemical species, and γ_X is its corresponding activity coefficient, which can be estimated using the extended Debye-Hückel equation for low ionic strength solutions (usually less than 1.0, which corresponds to a salinity of 55,000 mg/l). In the above relations, the K_i are the equilibrium constants for each reaction and vary with temperature and pressure. Thus, on the basis of the concentration of carbonate and bicarbonate ions in a non-reactive environment and knowing the measurements of temperature and pressure, it is possible to estimate the total carbon content in a water sample.

For calculation of the total inorganic carbon, the temperature and pressure can be reasonably estimated for in situ conditions [39]. The water composition, pH, CO_3, HCO_3 and alkalinity at depth are much more difficult to evaluate because formation water samples are analyzed at surface conditions, most often long after sampling by which time a large proportion of the dissolved gases have been lost. Thus, the simplest approach is to assume, nevertheless, that there were no changes in the carbon content of the water sample between the in situ and laboratory conditions. In this case, the carbon content at in situ conditions is assumed to be the same as at the surface, calculated on the basis of the CO_3^{2-} and HCO_3^- determinations at laboratory conditions using the above procedure and equilibrium constants, which for standard conditions (25 °C and atmospheric pressure) are: $K_1 = 10^{-6.3}$ and $K_2 = 10^{-10.3}$.

A more realistic assumption is to consider that the formation water sample was originally in geochemical equilibrium with the formation rocks, particularly with carbonate minerals such as calcite or dolomite (most likely calcite), owing to the very rapid equilibration of water with these minerals. Thus, if the rock mineralogy is known, geochemical speciation models can be used to bring the composition of the sampled formation waters up to in situ conditions, resulting in more accurate values for pH, CO_3^{2-} and HCO_3^-. Both scenarios have been calculated here.

4. Maximum CO_2 saturation

The CO_2 solubility in pure water depends on pressure and temperature. The mole fraction of CO_2 at saturation in fresh water, $x_{w,S}^{CO_2}$, can be calculated according to the Krichevsky–Kasarnovsky equation [40]:

$$\ln\left(\frac{f_{CO_2}}{x_{w,S}^{CO_2}}\right) = \ln H_{CO_2}^* + \frac{\bar{v}_{CO_2}^{\infty}}{RT}P_{aq} \tag{4}$$

where f_{CO_2} is the fugacity of pure phase CO_2, $\bar{v}_{CO_2}^{\infty}$ is the molar volume of CO_2 at infinite dilution, T is temperature in K, $R = 8.314$ (J mol^{-1}K^{-1}) is the universal gas constant, P_{aq} is pressure in the water rich phase (MPa) and $H_{CO_2}^*$ is the reference Henry's constant. Using a very large volume of experimental data from the literature, Enick and Klara [40] developed the following relations for the reference Henry's constant and molar volume of CO_2 at dilution, valid in the temperature range 298–523 K (25–250 °C) and from 3.4 to 72.4 MPa:

$$H_{CO_2}^* = -5032.99 + 30.741113T - 0.052667T^2 + 2.630218 \times 10^{-5}T^3 \tag{5}$$

$$\bar{v}_{CO_2}^{\infty} = 1799.36 - 17.8218T + 0.0659297T^2 - 1.05786 \times 10^{-4}T^3 + 6.200275 \times 10^{-8}T^4 \tag{6}$$

The fugacity f_{CO_2} of the pure phase CO_2 is calculated from equations of state [41].
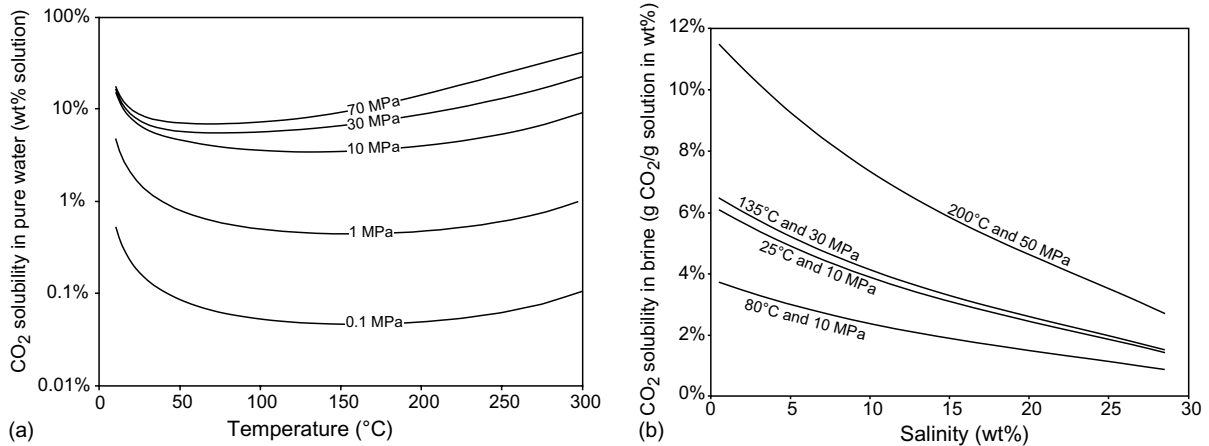
Fig. 1. Variation of CO_2 solubility in water: (a) with temperature and pressure; and (b) with salinity, for various conditions representative of sedimentary basins.

Fig. 1a shows the dependence of CO_2 solubility on temperature T and pressure P for the ranges found in sedimentary basins, calculated according to Eqs. (4)–(6). It is worth noting that for a given pressure, the CO_2 solubility in water decreases with increasing temperature at low temperatures, with a decreasing slope as temperature increases, and after reaching a minimum, it increases to values that, for high temperatures and pressures, may be higher than the solubility at low temperatures. The minimum solubility is reached for lower and lower temperatures as the pressure increases (Fig. 1a). Also, the rate of increase in solubility with pressure decreases significantly as the pressure increases. This behavior is due to the properties of CO_2 [41].

Formation waters contain dissolved solids, and their presence decreases the solubility of light gases such as CO_2 (salting out effect). Enick and Klara [40] used a data set of 167 solubility values for the same temperature range of 298–523 K and pressures from 3 to 85 MPa to obtain the following correlation between CO_2 solubility at saturation in saline water, X (in mass fraction), and water salinity S (total dissolved solids, TDS, in wt.%):

$$X_{b,S}^{CO_2} = X_{w,S}^{CO_2}(1.0 - 4.893414 \times 10^{-2}S + 0.1302838 \times 10^{-2}S^2 + 0.1871199 \times 10^{-4}S^3) \qquad (7)$$

which indicates a fivefold decrease in CO_2 solubility in brine for an increase in salinity from 0% to 30%. There are other relations in the literature for CO_2 solubility in brines [42], but the Enick and Klara [40] relations are the most complete and cover the broadest spectrum of temperatures and pressures as found in sedimentary basins. The strong effect of salinity on CO_2 solubility in formation water is illustrated in Fig. 1b.

Thus, if the in situ characteristics of the formation water (pressure, temperature and salinity) are known, the maximum CO_2 content at saturation can be estimated using Eqs. (4)–(7). The only additional parameter that needs to be estimated for determination of the ultimate CO_2-sequestration capacity in solution in an aquifer is the formation water density.

5. Density of formation water containing CO_2

To calculate the current carbon content in the formation water and at saturation, one needs to estimate the density of water containing CO_2. The density of fresh water increases only slightly (<3%) when CO_2 is dissolved, and the solubility of CO_2 decreases significantly when other ions are present in solution [40], Eq. (7) above. By comparison with the increase in density of the formation water when salinity increases, the contribution of dissolved gases, including CO_2, is very small and usually is neglected. Hence, there are no relations in the literature for calculating the density of formation water containing CO_2.

The density of pure water, ρ_w, decreases with increasing temperature and increases to a much lesser extent with increasing pressure. The density of formation water increases significantly with increasing salinity, by as much as 30% for saturated brines (40% mass fraction dissolved solids). After analyzing several published algorithms for calculating water density, Adams and Bachu [43] reached the conclusion that the following expressions, presented by Batzle and Wang [44], best describe the fresh and saline water density for the ranges of temperature 20–350 °C, pressure 5–100 MPa and salinities up to 320,000 mg/l, without significant computational effort:

$$\rho_w = 1 + 1 \times 10^{-6}(-80T - 3.3T^2 + 0.00175T^3 + 489P - 2TP + 0.016T^2P$$
$$- 1.3 \times 10^{-5}T^3P - 0.333P^2 - 0.002TP^2) \tag{8}$$

$$\rho_b = \rho_w + S\{0.668 + 0.44S + 1 \times 10^{-6}[300P - 2400PS$$
$$+ T(80 - 3T - 3300S - 13P + 47PS)]\} \tag{9}$$

where T is temperature in °C, P is pressure in MPa, S is salinity in mass fraction (ppm/10^6) and ρ_w and ρ_b are fresh water and brine density values, respectively, in g/cm^3.

Dissolved CO_2 has the effect of increasing water density, by up to 2–3% in the temperature range of 5–300 °C [42,45]. For ideal solutions, it is assumed that the partial molar volumes of the species in solution are equal to the volumes of the pure species at the same temperature and pressure, in which case the total volume of the solution, V_T, is given by:

$$V_T = n_1 v_1 + n_2 v_2$$

where n is the number of moles, v is specific molar volume (m^3/mol) and the subscripts 1 and 2 stand for the two species. Expressing the molar volume in terms of density $\rho = M/v$, where M is molar mass (kg/mol) and taking into account that the total mass M_T is the sum of the individual components ($M_T = n_1 M_1 + n_2 M_2$) leads to the following expression for the density ρ of the solution:

$$\frac{1}{\rho} = \frac{X_1}{\rho_1} + \frac{X_2}{\rho_2} \tag{10}$$

which is the harmonic mean of the densities of the two components. In Eq. (10), $X_i = n_i M_i/(n_1 M_1 + n_2 M_2)$ is the mass fraction of the species i ($i = 1, 2$).

For CO_2 saturated water, the application of Eq. (10) leads to density values much lower than the density of pure water, contrary to the observed actual increase in density for CO_2 bearing water when dissolving CO_2. For example, according to Eq. (10), the density of water containing

2.58% CO_2 at a temperature of 20 °C and pressure of 9.87 MPa would be 998.18 kg/m^3, compared with a measured density of 1014.80 [42]. Obviously, an aqueous CO_2 solution is not ideal, and the use of Eq. (10) leads to erroneous results.

For non-ideal solutions, it is assumed that the solvent (water in this case) contributes the same molar volume as in the pure state, while the solute contributes only an apparent molar volume V_ϕ:

$$V_T = n_1 v_1 + n_2 V_\phi$$

Expressing the apparent partial molar volume, V_ϕ, in terms of density values and molecular weights [42] and after some manipulation, the following expression is obtained for the density of the aqueous solution [45]:

$$\rho_{aq} = \rho_w + M_2 \cdot c - c\rho_w \cdot V_\phi \tag{11}$$

where M_2 is the molecular weight of the solute ($M_2 = 44.01$ g/mol for CO_2) and c is the solute molar concentration in mol/m^3 of solution. In practice, the molar concentration c is not known, but dimensional analysis shows that:

$$M_2 \cdot c = X_{sol} \cdot \rho_{aq}$$

where X_{sol} is the solute mass fraction. Use of the above relation in Eq. (11) leads, after some manipulation, to the following expression for the density of an aqueous solution of a single solute dissolved in pure water when the mass fraction, X_{sol}, is known:

$$\rho_{aq} = \frac{\rho_w}{1 - X_{sol}\left(1 - \frac{V_\phi}{M_2}\rho_w\right)} \tag{12}$$

Since the density of the aqueous solution is greater than that of pure water, Eqs. (11) and (12) indicate that the following condition must always be satisfied:

$$V_\phi < \frac{M_2}{\rho_w} \tag{13}$$

Published experimental results, reviewed by Garcia [45], show that the apparent molar volume for CO_2 is weakly dependent on the CO_2 mole fraction and is negligibly dependent on pressure for temperatures below 300 °C. On the basis of 53 data points, Garcia [45] proposes the following expression for the apparent molar volume of CO_2:

$$V_\phi = 37.51 - 9.585 \times 10^{-2}T + 8.740 \times 10^{-4}T^2 - 5.044 \times 10^{-7}T^3 \tag{14}$$

This expression for V_ϕ satisfies Eq. (12) in the case of CO_2 dissolved in pure water.

A straight forward use of Eq. (12) by replacing the pure water density ρ_w with brine density ρ_b is not acceptable because it would violate Eq. (13), as the water density increases with increasing salinity. Following the approach of Batzle and Wang [44] with regard to the density of formation water containing dissolved solids, one can calculate first the density of pure water containing CO_2 using Eqs. (8), (12) and (14) above and then correct it to account for the formation water salinity. No method has been presented to date for applying a salinity correction to waters containing CO_2 in solution. Thus, three different possible approaches are being suggested and discussed in the following.

Case 1: Scaling of the density of CO_2 bearing brine by freshwater density

The simplest approach would be to scale the brine density, ρ_b, by considering that the density of brine containing CO_2, $\rho_b^{CO_2}$, increases by the same ratio as the density of pure water:

$$\rho_b^{CO_2} = \frac{\rho_w^{CO_2}}{\rho_w} \rho_b \qquad (15)$$

where $\rho_w^{CO_2}$ is the density of pure water containing CO_2. The major flaw of this approach is that it does not take into account the decrease in CO_2 solubility and apparent molar volume with increasing salinity. Use of this scaling method will increasingly overestimate the density of formation water saturated with CO_2 as the salinity increases.

Case 2: Scaling of the apparent molar volume by solubility

To account fully for the decrease in CO_2 solubility with increasing salinity, the CO_2 solubility in formation water can be calculated using Eq. (7), and the apparent molar volume of CO_2 should be reduced with increasing salinity in a manner that will satisfy Eq. (13). In this case, the density of CO_2 saturated formation water can be calculated directly by substituting ρ_b for ρ_w in Eq. (12). Unfortunately, there are no data that would allow the derivation of an empirical expression for the decrease in the apparent molar volume similar to Eq. (14). One possible approach is to consider empirically that the apparent molar volume, V_ϕ^b, for CO_2 dissolved in brine decreases with increasing salinity by the same ratio as the decrease in solubility:

$$V_\phi^b = \frac{X_{b,S}^{CO_2}}{X_{w,S}^{CO_2}} V_\phi \qquad (16)$$

While the use of this relation satisfies Eq. (13), the decrease in the CO_2 apparent molar volume with salinity is quite significant, dropping below 10 cm³/mol for high salinity (Fig. 2). Although the amount of CO_2 in solution continuously decreases with increasing salinity, the difference in
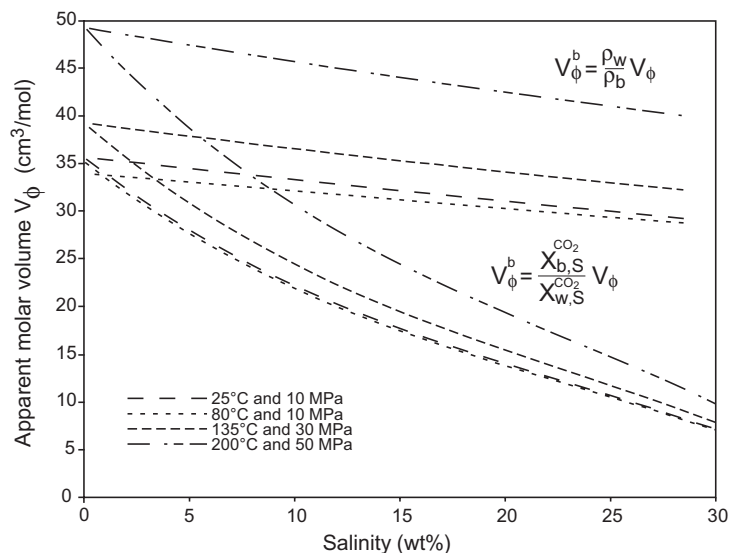

Fig. 2. Variation with salinity of the CO_2 apparent molar volume, V_ϕ, assuming proportionality with either CO_2 solubility in brine, $X_{b,S}^{CO_2}$, or with brine density ρ_b, for conditions characteristic of sedimentary basins.
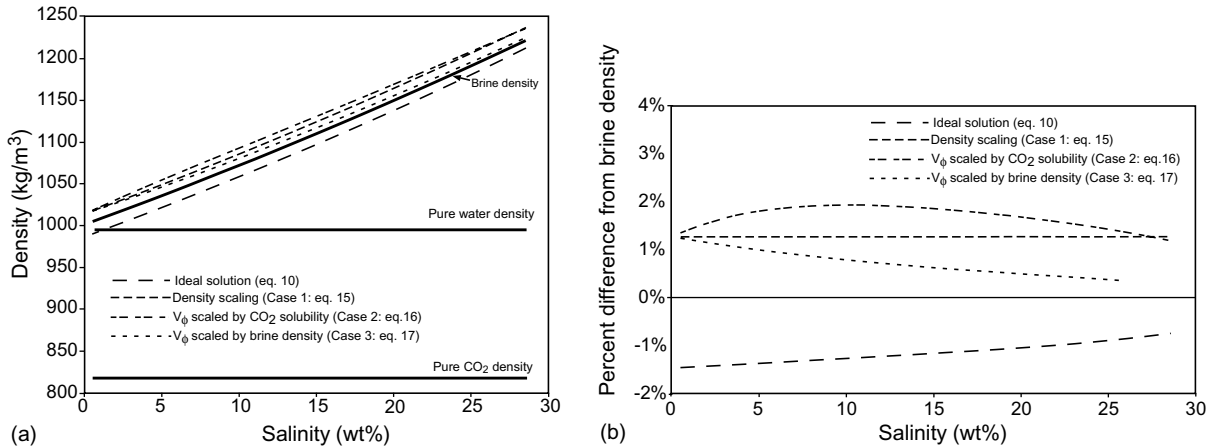
Fig. 3. Variation with salinity of the density of water containing dissolved CO_2 for $T = 25$ °C and $P = 10$ MPa, compared with freshwater, brine and CO_2 density ($\rho_{CO_2} = 817.63$ kg/m³), calculated using various mixing algorithms: (a) absolute values; and (b) percent difference from brine density.

density between the CO_2 saturated and CO_2 free formation water increases with increasing salinity till approximately 10 wt.% and then decreases, rather than espousing the expected behavior of a monotonic decrease (Fig. 3).

Case 3: Scaling of the apparent molar volume by density

An increase in water salinity, hence the number of ions in solution, clearly reduces the ability of the solvent to accept additional CO_2 ions, thus the reduction in CO_2 solubility. However, while the number of CO_2 moles that could dissolve decreases, the mass of any particular number of moles remains constant, be they dissolved in pure or formation water, regardless of the water salinity. This mass conservation principle leads to the relation:

$$V_\phi^b \rho_b = V_\phi \rho_w \tag{17}$$

Use of Eq. (17) in Eq. (12) automatically assures Eq. (13) and makes straight forward the calculation for CO_2 saturated formation water. The apparent molar volume of CO_2 decreases less drastically than in the case of Eq. (16) (Fig. 2), and the difference between the density of the CO_2 saturated and CO_2 free formation water decreases monotonically with increasing salinity, as expected (Fig. 3).

Using Eqs. (3)–(9), (12), (14) and (17), the current total inorganic carbon content present in formation water and the maximum CO_2 at saturation and the corresponding density of formation water can be determined at every point in an aquifer. It is then possible to calculate the ultimate capacity for CO_2 sequestration in solution in an aquifer or any region thereof using Eq. (2) and standard mapping procedures.

6. Example of application: the Viking Aquifer in the Alberta basin

The Alberta sedimentary basin in western Canada (Fig. 4a) is a large petroleum producer. Notwithstanding the decrease in CO_2 emissions per unit of output, such as per barrel of produced
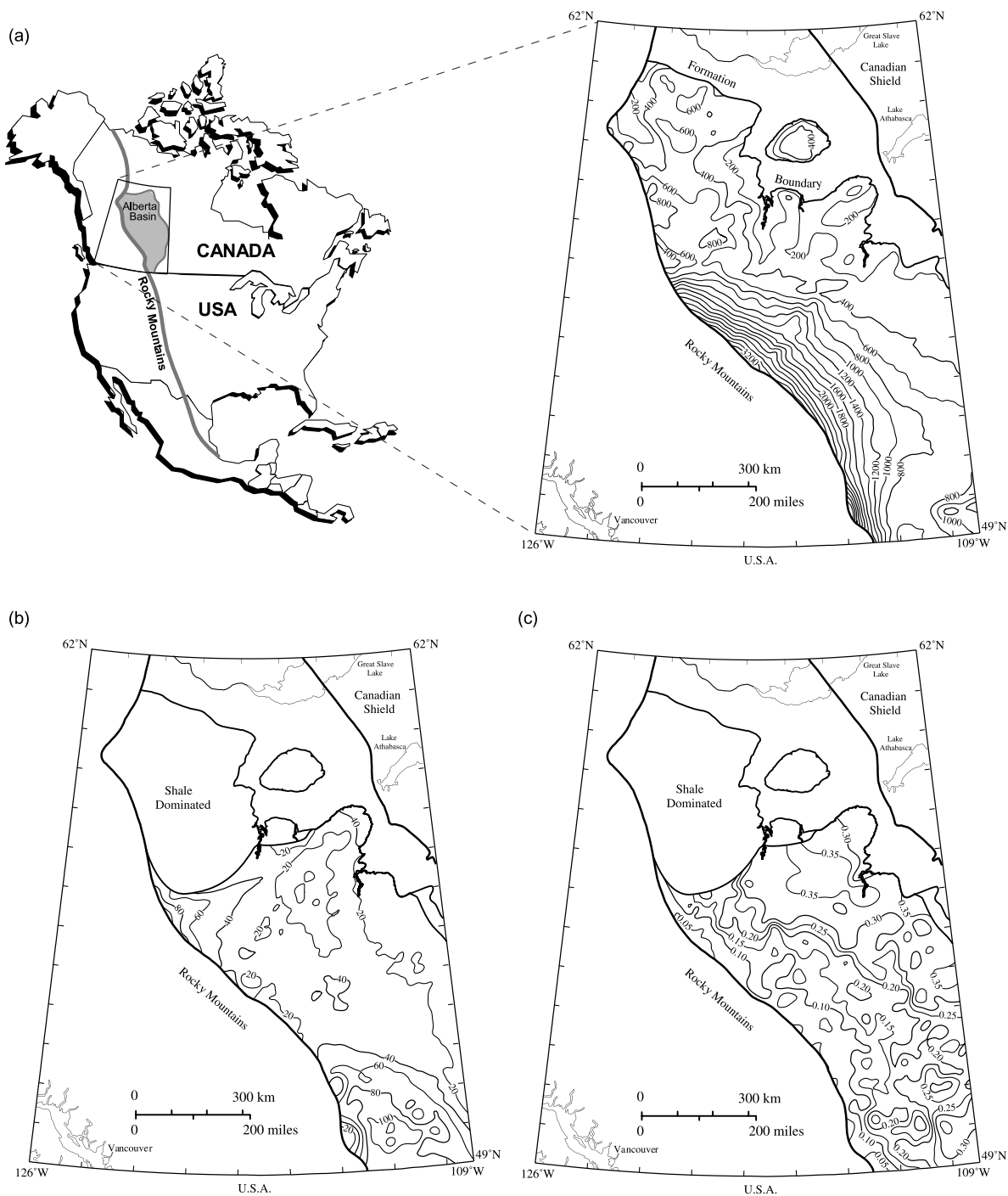
Fig. 4. Characteristics of the Viking formation, Alberta basin, Canada: (a) depth (m) to structure top; (b) thickness (m); and (c) porosity (fraction).

oil, CO_2 emissions have increased by more than 25% since 1990 due to both population increase and economic growth in the basin. In addition, unlike many other regions in North America, most of the CO_2 is produced at large, stationary point sources, such as thermal power plants, refineries, oil sands, petrochemical and cement plants and pulp mills. Approximately 60% of the CO_2 emissions in the basin, at 208 Mt/year in 1999 the highest in Canada, are produced at such sources, each greater than 100 kt/year. The Alberta basin is generally well suited for CO_2 geological sequestration because CO_2 can be sequestered or stored by all means and it meets all the basin scale criteria, such as tectonic stability, favorable geology and hydrogeology, abundance of oil and gas reservoirs, presence of extensive coal and salt beds, maturity and well developed infrastructure [46]. In the basin, CO_2 geological sequestration must play a major role in reducing CO_2 emissions because ocean sequestration is not an option for a landlocked sedimentary basin like Alberta, and terrestrial sequestration is providing little capacity in a region where agriculture and forestry are important industries.

Oil reserves in the Alberta basin are in decline, and gas reserves recently reached their peak, such that approximately 5600 oil pools and 5300 gas pools are depleted and abandoned, out of 9128 and 30,600, respectively. The estimated sequestration capacity of depleted oil and gas pools, currently on the order of 300 Mt CO_2, is insufficient to cover immediate CO_2 sequestration needs, even if additional oil and gas pools reach depletion in the next few years. Enhanced oil and methane recovery, although an option, are still in the stage of implementation and technological development, respectively. Thus, CO_2 sequestration in deep saline aquifers is likely to be implemented in the Alberta basin concurrently with other sequestration means.

The Alberta basin, covering a surface of approximately 780,000 km^2, forms a wedge of sedimentary rocks of approximately 1,681,000 km^3 that thickens from zero in the northeast at the Canadian Precambrian Shield to more than 6000 m in the southwest at the edge of the thrust and fold belt of the Rocky Mountains. It contains a succession of carbonate and sandstone units that form aquifers, separated by intervening shales and evaporitic rocks that form aquitards and aquicludes. The Viking aquifer was chosen to develop the methodology for estimating the capacity for CO_2 sequestration in solution in deep saline formation waters because this aquifer: (1) hosts formation waters that are moderately saline (reduces the salting out effect), (2) is capped by the tight and regionally extensive Colorado aquitard and (3) has the potential for enhanced hydrodynamic trapping of CO_2 in a downdip, inward flow system driven in the western part of this aquifer by erosional rebound in the adjacent shales [23,47].

The lower cretaceous Viking formation, covering an area of 647,600 km^2 (Fig. 4a), was deposited in a marine environment and comprises mostly sandstone rocks, except for the northern part of the basin, where it is shaly. The sandstones are composed of 76–98% quartz and contain minor amounts of clay minerals, iron oxides, feldspars, glauconite and carbonates. The carbonate fraction, as high as 10%, consists of ankerite and calcite. The formation, absent due to erosion in the northeast, dips from zero at outcrop in the north–northeast, to more than 3000 m depth in the southwest (Fig. 4a). The sandstone dominated portion of the formation has an average thickness of 31 m, although in the south and in the northwest, it reaches as high as 120 m (Fig. 4b) and represents only a minuscule 0.64% of the rock mass of the Alberta basin. Because of differential compaction, well scale porosity varies in the Viking aquifer from less than 5% at its deepest in the southwest to more than 35% at its shallowest in the northeast (Fig. 4c).

The pore space in the Viking Formation is saturated with saline water, except for the deep portion adjacent to the thrust and fold belt, where it is saturated mainly with gas as a result of continuing gas generation in the deep basin [48]. The Viking aquifer is defined by the water saturated region of the sandstone dominated Viking Formation and covers an area of 503,670 km^2. Relevant properties of the formation water and injected CO_2 at in situ conditions were calculated according to the procedure described by Bachu [39] on the basis of 3525 good quality drill stem tests and 2875 water analyses, the latter being the result of an extensive quality checking and culling process using the methods presented by Hitchon and Brulotte [49] and Hitchon [50]. Temperature and pressure at the top of the Viking aquifer, controlled mainly by depth, vary from surface conditions at outcrop (5 °C and 200 kPa at 10 m depth) to more than 70 °C and 18 MPa at its deepest in the west (Fig. 5a and b). Water salinity is low, less than 10,000 mg/l, in the recharge areas in the south and northwest and at discharge in the northeast, where fresh meteoric water enters the aquifer. The salinity reaches more than 80,000 mg/l in a large saline plume in the central area of the aquifer (Fig. 5c). Water density, calculated using a direct regression line relationship [43] because the relationship of Batzle and Wang [44], does not fit waters in the Alberta basin [43], varies between less than 1000 kg/m^3 in shallow, low salinity areas to more than 1060 kg/m^3 at the center of the high salinity plume (Fig. 5d).

The injected CO_2 will be a dense fluid (liquid or supercritical, Fig. 6a) at depths greater than 1200 m, except in the south where it will be a liquid starting at depths slightly greater than 600 m (compare Figs. 6a and 4a) as a result of the "cold basin" characteristics of the Alberta basin [39,46]. The region that meets the criteria for CO_2 injection [51,52] covers an area of 209,700 km^2 in the south and west (Fig. 6a). In this area, the CO_2 density at in situ conditions varies between 250 kg/m^3 and more than 750 kg/m^3 (Fig. 6b). Because the density of the dense fluid CO_2 decreases, rather than increases, with depth in a cold basin [39], the highest CO_2 density is attained in the southern part of the basin at shallower depths, where CO_2 is a liquid, rather than at greater depths in the western part of the basin, where CO_2 is in a supercritical state.

6.1. Capacity calculations

To calculate the capacity for dissolved phase CO_2 in Viking formation waters, the difference between the maximum solubility of CO_2 and the current inorganic carbon content in the reservoir was determined using three methods. Further culling of the data set of formation water analyses, used to map the formation water salinity, removed all those with missing pH values or having a charge balance difference greater than 12%. This left 2569 analyses for total inorganic carbon (TIC), maximum CO_2 solubility and capacity calculations. The in situ temperature and pressure conditions were calculated at the collection point of each water sample.

For TIC calculations, the aquifer was assumed to contain no non-carbonate buffers and to be non-reactive because the water analyses in the Viking aquifer document only major ion concentrations, TDS values and pH at laboratory conditions. Based on these assumptions, the simplest way to calculate TIC would be to determine the equilibrium carbonate concentrations at laboratory conditions as a proxy for in situ conditions, using the extended Debye-Hückel equation as described in the Current Carbon Content section. To test the validity of this approach, the current TIC was then calculated for in situ conditions, using the speciation geochemical model SolminDB, which is a modified version of Solmineq [53], able to perform calculations in a
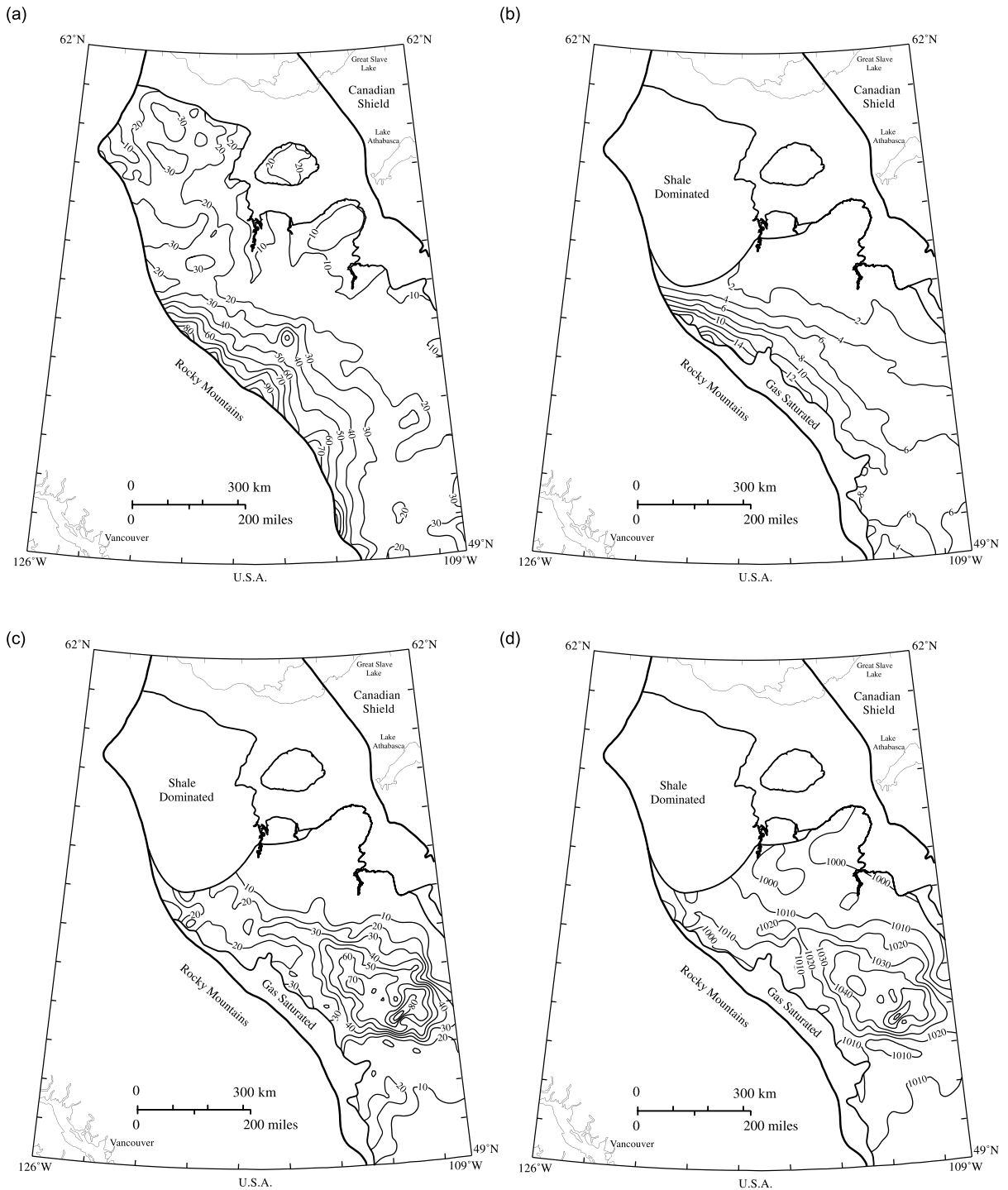
Fig. 5. Characteristics of formation waters in the Viking aquifer, Alberta basin, Canada: (a) temperature (°C); (b) pressure (MPa); (c) salinity (g/l); and (d) density (kg/m³).
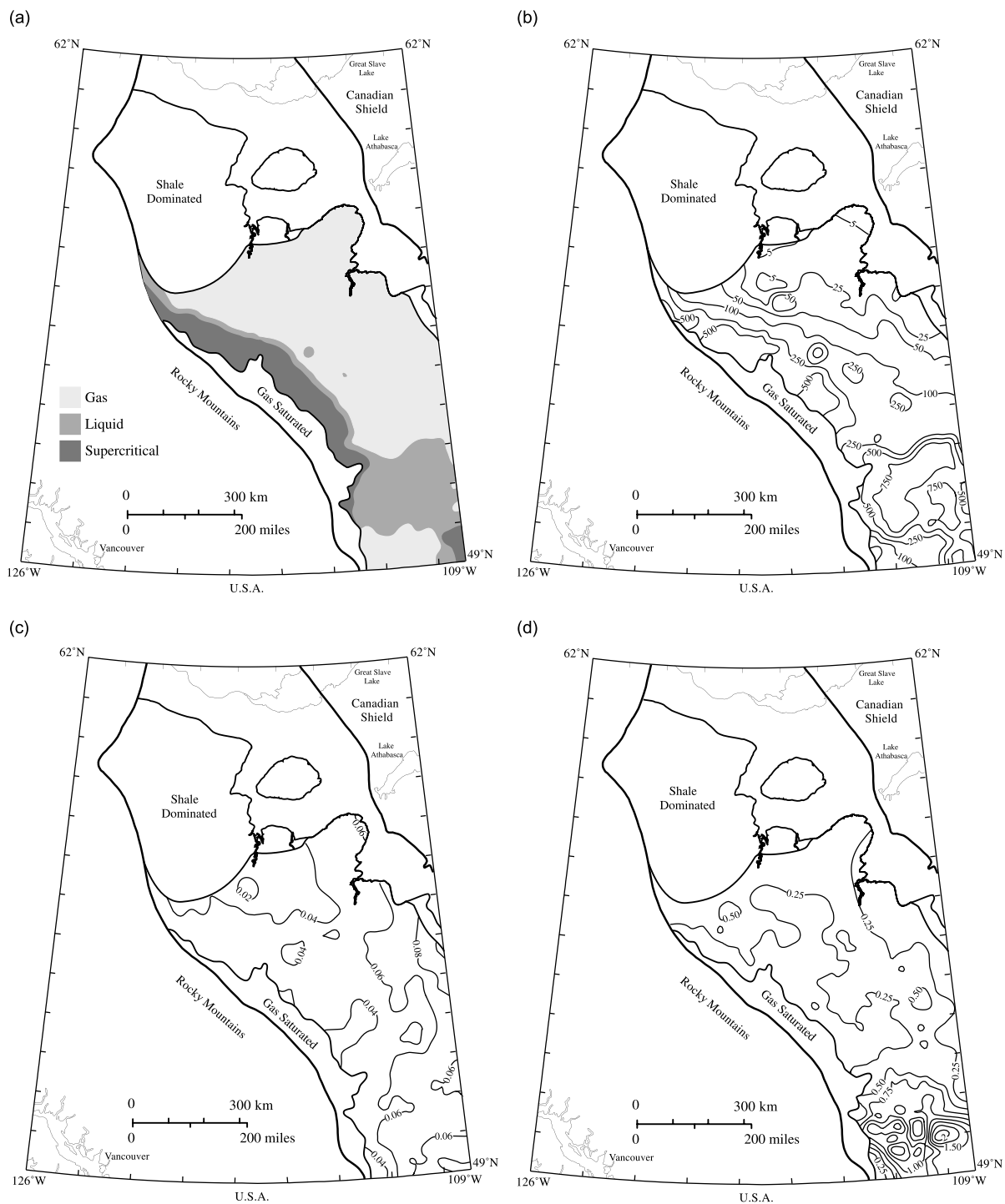
Fig. 6. Estimated characteristics of CO_2 if injected in the Viking aquifer, Alberta basin, Canada: (a) phase distribution; (b) density (kg/m^3); (c) maximum solubility (g CO_2/g brine); and (d) sequestration capacity (t CO_2 /m^2 aquifer, or Mt CO_2/km^2).

database. For this scenario, each water sample was brought to in situ conditions assuming equilibrium with the calcite present in the cements in the rock matrix and validity of the extended Debye-Hückel equation. However, more than 500 analyses have ionic strengths greater than 1 (equivalent to a salinity of ~58,000 mg/l $NaCl_{(aq)}$), which is the practical limit of the extended Debye-Hückel equation [53]. These high salinity formation waters may require the use of Pitzer equations for calculating the effective concentration of dissolved salts to represent the system more accurately. Thus, a third set of calculations was run assuming in situ conditions and equilibrium with calcite using the Pitzer equations in SolminDB [53]. The results of all of these calculations are presented in Table 1.

As expected, the values of the current TIC are higher, by two orders of magnitude in this case, for low salinity water than for the high salinity water, using the Debye-Hückel equation. The current TIC is also higher when in situ conditions are taken into account than when the TIC at in situ is considered the same as at the surface, due to the loss of dissolved gases during sampling and transportation. The difference between the current TIC at surface and at in situ conditions, when calculated using the Debye-Hückel equations, varies between −215% and 29%, with an average of −18.2% and a standard deviation of 25%. For saline waters, the Pitzer equations more accurately determine activity coefficients and are limited only by the availability and range of laboratory data for individual species (temperatures generally less than 75 °C). The results using Pitzer equations for Viking waters are very similar to the Debye-Hückel derived solution. Only 120 samples out of 2569 generated TIC values more than 5% different than the Debye-Hückel solution, and all of these samples had ionic strengths greater than the theoretical limit of validity for the Debye-Hückel equation. The Pitzer equations consistently predict slightly greater TIC values than the Debye-Hückel derived values, which may be due to the fundamental differences in the models or the background data. An alternative explanation may be that as ionic strength increases past its theoretical limit, Debye-Hückel activity coefficients continue to decrease, whereas Pitzer values begin to increase according to experimental observations. For the Viking aquifer, the point average and areal averages of the Pitzer derived data reflect the higher TIC values but by only 2.8% of the Debye-Hückel derived TIC averages. Since the results are obstensibly the same and the Pitzer routines are far more computationally intensive, the Debye-Hückel equation is the preferred solution for water of moderate ionic strength.

Table 1
Comparison in the current total inorganic carbon (TIC) in the Viking aquifer, Alberta basin, Canada, calculated using different geochemical models and assuming surface and in situ equilibrium conditions

Label and geochemical model	Calculation conditions	Minimum	Maximum	Point average	Areal average
Current TIC (mg CO_2/g solution)					
DH1 (Debye-Hückel)	Surface	0.044	2.97	0.61	0.59
DH2 (Debye-Hückel)	In situ	0.042	4.80	0.77	0.70
P (Pitzer)	In situ	0.044	5.06	0.79	0.72
Percent difference (DH1-DH2)/DH1*100	–	4.9%	−62%	−26%	−20%
Percent difference (DH2-P)/DH2*100	–	−5.3%	−5.3%	−2.8%	−2.8%

The change in TIC from surface to in situ conditions leads to a slight increase in salinity and affects accordingly the density of formation waters. However, this effect is marginal, such that the percent differences in TIC per unit volume of solution between the various methods of calculating TIC are the same as for the TIC per unit mass of solution. Similarly, the change in salinity from surface to in situ conditions leads to a corresponding slight change in CO_2 solubility at saturation for the 2659 data points, which were calculated for the various cases (surface and in situ salinity) using Eqs. (4)–(7) for the in situ aquifer temperature and pressure conditions (Fig. 5a and b). Again, the difference is small, practically negligible (between −1.2% and 1.8%, with an average of 0.15% and standard deviation of 0.17%). Table 2 presents the calculated current TIC and maximum CO_2 solubility for in situ conditions calculated using the Debye-Hückel geochemical model.

The ultimate CO_2 capacity in solution in formation water in the aquifer was calculated for each analysis point using Eqs. (2), (8), (11) and (17) on the basis of current and maximum CO_2 in solution and water temperature, pressure and salinity (Fig. 5). Calculations were performed assuming both surface and in situ conditions and using both geochemical speciation models (Debye-Hückel and Pitzer). The differences in the results of the various cases are small (0.5% on average). For this reason, only the case of in situ conditions determined using the Debye-Hückel model is presented in Table 2.

The most important observation is that for this aquifer, the difference between the current and maximum TIC is approximately two orders of magnitude. As a result, the UCSCS is determined mainly by the maximum CO_2 solubility at saturation in the formation water and depends negligibly on the current total inorganic carbon. Thus, a large difference in the current TIC calculated by various methods (Table 1) translates, nevertheless, into only very small differences in capacity. Hence, in this and similar cases, achieving great accuracy in estimating the current TIC is not critical, particularly if the data are incomplete or the computational effort is significant. This situation may be completely different if the current TIC of the water is closer to saturation with CO_2. Fig. 6c presents the variation in the UCSCS in the formation water of the Viking aquifer.

Finally, the capacity of the entire Viking aquifer to sequester CO_2 dissolved in formation water is calculated considering its porosity and thickness (Fig. 4c and d). Results are presented in Table 2 and Fig. 6d. The capacity of formation waters in the Viking aquifer to sequester CO_2 in solution varies between 0.06 and 2.13 Mt CO_2/km^2 aquifer, with an areal average of 0.39 Mt CO_2/km^2. The ultimate CO_2 sequestration capacity in solution in the Viking aquifer, UCSCS, is 198.7 Gt CO_2. If surface rather than in situ conditions were considered, the calculated ultimate capacity would

Table 2
Capacity of the Viking aquifer, Alberta basin, Canada, to sequester CO_2 dissolved in formation water at in situ conditions

Type of capacity calculation	Minimum	Maximum	Point average	Areal average
Current TIC (kg CO_2/m^3 solution)	0.04	4.91	0.79	0.72
Maximum CO_2 solubility (kg CO_2/m^3 solution)	24.10	99.82	55.59	54.10
CO_2-sequestration capacity in solution (kg CO_2/m^3 solution)	24.06	99.10	54.81	53.68
Rock capacity (kg CO_2/m^3 rock)	1.46	34.41	10.67	13.95
Aquifer capacity (t CO_2/m^2, or Mt CO_2/km^2 aquifer)	0.06	2.13	0.57	0.39

have been 197.9 Gt CO_2, for a difference of only -0.4%. If the current TIC is completely neglected in the calculations and only the CO_2 solubility at saturation is considered, then the capacity of the Viking aquifer to store CO_2 in solution is calculated to be 201.3 Gt CO_2, for a difference of $+1.3\%$. The differences between the various capacity estimates, with and without current TIC at surface and in situ conditions, are well within the errors introduced by data measurement, assumptions, algorithms and various extrapolations used in the estimates. The results clearly suggest that using geochemical modeling to bring the analyses of formation waters to in situ conditions is not warranted when the current total inorganic carbon in the aquifer water is so low by comparison with the CO_2 solubility at saturation. Furthermore, the current TIC may even be neglected in capacity calculations, although it has to be evaluated first, at least at several representative points in the aquifer for comparison with the CO_2 dissolved in the formation water at saturation.

The value of 198.7 Gt CO_2 assumes that CO_2 is dissolved to saturation everywhere in the Viking aquifer. If, for safety reasons, CO_2 is injected and dissolves to saturation only in the region where it will be a dense fluid (Fig. 5a), then the ultimate CO_2 sequestration capacity in solution in the Viking aquifer, UCSCS, is reduced to only 106.6 Gt CO_2, with an areal average of 0.51 Mt CO_2/km^2 aquifer. However, the remaining capacity of 92.1 Gt CO_2 in the shallower part of the Viking aquifer does not necessarily have to be discarded. Water can be pumped from the aquifer, mixed with CO_2 at the surface and re-injected into the aquifer, provided that more CO_2 is sequestered than produced during the pumping, mixing and injection operations.

This aquifer represents only 0.64% of the total rock mass of the Alberta basin and 0.88% of the rock volume of the basin suitable for CO_2 injection as a dense fluid [46]. Excluding approximately 45% of this rock mass because it comprises aquitards and aquicludes and applying another reduction of 40% because of the increase in formation water salinity with depth, this back-of-the-envelope evaluation shows that approximately 4000 Gt CO_2 can be ultimately sequestered in solution in the Alberta basin. Of course, these estimates have to be confirmed by an aquifer-by-aquifer analysis of the type presented here for the Viking aquifer.

7. Summary and conclusions

The trend in climate warming observed in the last century is attributed to the effect of greenhouse gases, such as CO_2, whose concentration in the atmosphere has increased significantly since the beginning of the industrial revolution, primarily as a result of fossil fuel use. Since fossil fuels will likely continue to be the major energy source for the major part of this century, anthropogenic CO_2 emissions into the atmosphere need to be reduced significantly in order to stabilize and, hopefully, reverse the climate warming trend. Geological sequestration of CO_2 is a means of reducing atmospheric emissions that is immediately available and technologically feasible. Among the various options for CO_2 geological sequestration, it is currently thought that deep saline aquifers provide the largest capacity as a result of their size and wide distribution by comparison with other geological media such as hydrocarbon reservoirs.

Carbon dioxide can be sequestered in deep aquifers by mineral precipitation as a result of geochemical reactions between the injected CO_2 and the formation water and rocks, by dissolution in formation water and as a free phase CO_2 plume. The time scale of the processes involved in the three sequestration mechanisms are quite different, such that they can be decoupled. As a

result, their sequestration capacity can, by and large, be assessed individually. The UCSCS of an aquifer is the difference between the ultimate capacity for CO_2 at saturation and the total inorganic carbon currently in solution in that aquifer and depends on water pressure, temperature and salinity.

An aqueous inorganic carbon system is controlled by CO_2 dissolution in the water and interactions with carbonate and siliciclastic minerals. Since there are no direct measurements of the total inorganic carbon, methodology has been developed to calculate the current carbon content in formation waters on the basis of standard analyses of formation waters collected by the energy industry during exploration for and production of hydrocarbons. Assuming non-reactive aquifer conditions, the current carbon content is evaluated on the basis of the concentration of carbonate and bicarbonate ions and with the relations between the activities of these species at equilibrium at the conditions prevalent in the aquifer. Because formation water samples are analyzed at surface conditions, the analyses were brought to in situ conditions using a geochemical speciation model to account for dissolved gasses that are lost from the water sample. Both the Pitzer and Debye-Hückel models were used to determine the activity coefficients. However, no significant difference in the calculated TIC values was found between these two solutions. The maximum CO_2 content at saturation in formation water was calculated by estimating the CO_2 content at saturation in pure water and applying an empirical correction that takes into account the decrease in CO_2 solubility with increasing water salinity.

Having estimated the current inorganic carbon content in formation water and at saturation, the UCSCS in an aquifer was calculated by considering the effect of dissolved CO_2 on formation water density, the aquifer thickness and porosity to account for the volume of water in the aquifer pore space and the mass of CO_2 dissolved in water currently and at saturation. A method to estimate the density of CO_2 containing brine was introduced by which the density of pure water containing CO_2 in solution is corrected for the presence of other ions in solution. Results obtained by this method are consistent with observed laboratory data.

The methodology developed for estimating the ultimate CO_2 sequestration capacity in solution in aquifers has been applied to the Viking aquifer in the Alberta basin in western Canada. This aquifer, covering a surface of 500,000 km^2 and with an average thickness of 31 m, represents 0.64% of the rock mass in the Alberta basin and reaches depths of more than 3000 m. The temperature, pressure and salinity in the Viking aquifer vary from surface conditions at outcrop to more than 70 °C, 18 MPa and 90,000 mg/l, respectively. Considering only the region of 210,000 km^2 where the injected CO_2 would be a dense fluid (liquid or supercritical), the capacity of the Viking aquifer to sequester CO_2 in solution in formation water is calculated to be 106 Gt. Simple estimates then indicate that the capacity of the Alberta basin to sequester CO_2 dissolved in formation waters at depths greater than 1000 m is on the order of 4000 Gt CO_2.

The differences between the various capacity estimates, with and without current TIC at surface and in situ conditions, are well within the error introduced by data measurement, assumptions, algorithms and various extrapolations used in the estimates. Thus, using geochemical models to bring the analyses of formation waters to in situ conditions is not warranted when the current total inorganic carbon in aquifer water is very small by comparison with the CO_2 solubility at saturation. Furthermore, in such cases, the current TIC may be altogether neglected.

References

[1] Bryant E. Climate process and change. Cambridge, UK: Cambridge University Press; 1997. p. 209.

[2] Jepma C, Munasinghe M. Climate Change Policy. New York, NY: Cambridge University Press; 1998. p. 331.

[3] Bajura RA. The role of carbon dioxide sequestration in the long term energy future. In: Fifth International Greenhouse Gas Technologies Conference, Cairns, Australia, Collingwood. VIC, AU: CSIRO Publishing; 2001. pp. 52–8.

[4] Turkenburg WC. Sustainable development, climate change, and carbon dioxide removal (CDR). Energy Convers Manage 1997;38:3–12.

[5] Liro C, Adams E, Herzog H. Modelling the release of CO_2 in the deep ocean. Energy Convers Manage 1992;33:667–75.

[6] Gunter WD, Wong S, Cheel DB, Sjostrom G. Large CO_2 sinks: Their role in the mitigation of greenhouse gases from an international, national (Canadian) and provincial (Alberta) perspective. Appl Energy 1998;61:209–27.

[7] Jackson RB, Banner JL, Jobbagy EG, Pockman WT, Wall DH. Ecosystem carbon loss with woody plant invasion of grasslands. Nature 2002;418:623–6.

[8] Aya I, Yamane K, Shiozaki K. Proposal of self sinking CO_2 sending system: COSMOS. Pergamon: Elsevier Science Ltd; 1999. p. 269–74.

[9] Stevens SH, Kuuskraa VA, Gale J. Sequestration of CO_2 in depleted oil and gas fields: global capacity, costs and barriers. In: Fifth International Greenhouse Gas Technologies Conference (GHGT-5), Cairns, Australia, Collingwood. VIC, AU: CSIRO Publishing; 2001. p. 278–83.

[10] Tsang CF, Benson SM, Kobelski B, Smith RE. Scientific consideration related to regulation development for CO_2 sequestration in brine formations. Environ Geolog 2002;42:275–81.

[11] Bachu S, Gunter WD. Acid gas injection in the Alberta basin, Canada: a CO_2 storage experience. In: Baines SJ, Worden RH, Gale J, editors. Geological storage of carbon dioxide for emissions reduction: technology. Geological Society special publication, in press.

[12] Moritis G. Worldwide EOR Survey. Oil Gas J 2002;100(15):43–7.

[13] Hitchon B, Gunter WD, Gentzis T, Bailey RT. Sedimentary basins and greenhouse gases: A serendipitous association. Energy Convers Manage 1999;40:825–43.

[14] Hendriks CA, Blok K. Underground storage of carbon dioxide. Energy Convers Manage 1993;34:949–57.

[15] Blunt M, Fayers FJ, Orr FM. Carbon dioxide in enhanced oil recovery. Energy Convers Manage 1993;34:1197–204.

[16] Gunter WD, Perkins EH, McCann TJ. Aquifer disposal of CO_2-rich gases: Reaction design for added capacity. Energy Convers Manage 1993;34:941–8.

[17] Gunter WD, Gentzis T, Rottenfusser BA, Richardson RJH. Deep coalbed methane in Alberta, Canada: A fuel resource with the potential of zero greenhouse emissions. Energy Convers Manage 1997;38:217–22.

[18] Dusseault M, Bachu S, Davidson B. Carbon dioxide sequestration in Alberta salt solution caverns. Solution Mining Research Institute, Fall 2001 Technical Meeting, Albuquerque, NM, 2001.

[19] Holtz MH, Nance PK, Finley RJ. Reduction of greenhouse gas emissions through CO_2 EOR in Texas. Environ Geosci 2001;8(3):187–99.

[20] Koide H, Yamazaki K. Subsurface CO_2 disposal with enhanced gas recovery and biochemical carbon recycling. Environ Geosci 2001;8(3):218–24.

[21] Gunter WD, Wiwchar B, Perkins EH. Aquifer disposal of CO_2-rich greenhouse gases: Extension of the time scale of experiment for CO_2 sequestering reactions by geochemical modeling. Mineralog Petrolog 1997;59:121–40.

[22] Gale J, Christensen NP, Cutler A, Torp TA. Demonstrating the potential for geological storage of CO_2: The Sleipner and GESTCO projects. Environ Geosci 2001;8(3):160–5.

[23] Bachu S, Gunter WD, Perkins EH. Aquifer disposal of CO_2: Hydrodynamic and mineral trapping. Energy Convers Manage 1994;35(4):269–79.

[24] IEA, GHGGP (International Energy Agency Greenhouse Gas R&D Programme). Carbon dioxide utilization. Stoke Orchard, Cheltenham, U.K.: IEA Greenhouse Gas R&D Programme; 1995.

[25] Holloway S, Savage D. The potential for aquifer disposal of carbon dioxide in the UK. Energy Convers Manage 1993;34:925–32.

[26] Baklid A, Korbøl R, Owren G. Sleipner Vest CO_2 disposal, CO_2 injection into a shallow underground aquifer. SPE Annual Technical Conference, Denver, CO, 1996. p. 269–77.

[27] van der Meer LGH. Investigations regarding the storage of carbon dioxide in aquifers in the Netherlands. Energy Convers Manage 1992;33(5–8):611–8.

[28] van der Meer LGH. Computer modeling of underground CO_2 storage. Energy Convers 1996;37(6–8):1155–60.

[29] Krom TD, Jacobsen FL, Ipsen KH. Aquifer based carbon dioxide disposal in Denmark: Capacities, feasibility, implications and state of readiness. Energy Convers Manage 1993;34(9–11):933–40.

[30] Korbol R, Kaddour A. Sleipner Vest CO_2 disposal injection of removed CO_2 into the Utsira Formation. Energy Convers Manage 1995;36:509–12.

[31] Law DH-S, Bachu S. Hydrogeological and numerical analysis of CO_2 disposal in deep aquifers in the Alberta sedimentary basin. Energy Convers Manage 1996;37:1167–74.

[32] Ispen KH, Jacobsen FL. The Linde structure, Denmark, an example of a CO_2-depository with a secondary chalk cap rock. Energy Convers Manage 1996;37(6–8):1161–6.

[33] McPherson BJOL, Cole BS. Multiphase CO_2 flow, transport and sequestration in the Powder River basin, Wyoming, USA. J Geochem Explor 2000;69–70:65–70.

[34] Holt T, Jensen JI, Lindeberg E. Underground storage of CO_2 in aquifers and oil reservoirs. Energy Convers Manage 1995;36(6-9):535–8.

[35] Koide HG, Tazaki Y, Noguchi Y, Nakayama S, Iijima M, Ito K, et al. Subterranean containment and long-term storage of carbon dioxide in unused aquifers and in depleted natural gas reservoirs. Energy Convers Manage 1992;33(5–8):619–26.

[36] Bergman PD, Winter EM. Disposal of carbon dioxide in aquifers in the US. Energy Convers Manage 1995;36(6–9):523–6.

[37] Bradshaw J, Rigg A. The GEODISC program: research into geologic sequestration of CO_2 in Australia. Environ Geosci 2001;8(3):166–76.

[38] Koide HG, Takahashi M, Tsukamoto H. Self-trapping mechanisms of carbon dioxide. Energy Convers Manage 1995;36(6–9):505–8.

[39] Bachu S. Sequestration of CO_2 in geological media in response to climate change: roadmap for site selection using the transform of the geological space into the CO_2-phase space. Energy Convers Manage 2002;43:87–102.

[40] Enick RM, Klara SM. CO_2 Solubility in water and brine under reservoir conditions. Chem Eng Commun 1990;90:23–33.

[41] Span R, Wagner W. A new equation of state for carbon dioxide covering the fluid region from the triple-point temperature to 1100 K at pressures up to 800 MPa. J Phys Chem Ref Data 1996;25:1509–96.

[42] Teng H, Yamasaki A, Chun MK, Lee H. Solubility of liquid CO_2 in water at temperatures from 278 K to 293 K and pressures from 6.44 MPa to 29.49 MPa and densities of the corresponding aqueous solutions. J Chem Thermodyn 1997;29:1301–10.

[43] Adams JJ, Bachu S. Equations of state for basin geofluids: Algorithm review and intercomparison for brines. Geofluids 2002;2:257–71.

[44] Batzle M, Wang Z. Seismic properties of pore fluids. Geophysics 1992;57(11):1396–408.

[45] Garcia JE. Density of aqueous solutions of CO_2. Report LBNL-49023 Lawrence Berkeley National Laboratory, CA 2001. 8 p.

[46] Bachu S, Stewart S. Geological sequestration of anthropogenic carbon dioxide in the Western Canada Sedimentary Basin Suitability analysis. J Canadian Petroleum Technol 2002;41(2):32–40.

[47] Bachu S, Gunter WD. Storage capacity of CO_2 in geological media in sedimentary basins, with application to the Alberta basin. Amsterdam: Pergamon, Elsevier Science Ltd; 1999. p. 195–200.

[48] Masters JA. In: Masters JA, editor. Elmworth—Case study of a deep basin gas field, 1984, p. 1–33.

[49] Hitchon B, Brulotte M. Culling criteria for standard formation water analyses. Appl Geochem 1994;9:637–45.

[50] Hitchon B. Rapid evaluation of the hydrochemistry of a sedimentary basin using only standard formation water analyses: Example from the Canadian portion of the Williston basin. Appl Geochem 1996;11:789–95.

[51] Bachu S. Sequestration of CO_2 in geological media: Criteria and approach for site selection in response to climate change. Energy Convers Manage 2000;41:953–70.

[52] Bachu S. Screening and ranking of sedimentary basins for sequestration of CO_2 in geological media in response to climate change. Environmental Geology. 44:277–289.

[53] Kharaka YK, Gunter WD, Aggarwal PK, Perkins EH, DeBraal JD. SOLMINEQ.88, A Computer Program for Geochemical Modeling of Water-Rock Interactions. US Geological Survey, Water-Resources Investigations Report 88-4277, 1989. p. 420.